Acta Cryst. (1971). A27, 148

The Evaluation of Thermal Diffuse Scattering of Neutrons for a One-Velocity Model

BY M. J. COOPER
Materials Physics Division, A.E.R.E. Harwell, Berkshire, England

(*Received* 19 *March* 1970)

The nature of the scattering surfaces for thermal diffuse scattering (TDS) and the contribution of TDS to the intensity measured during a scan through a Bragg reflexion are considered for a model in which all phonons are assumed to have the same velocity in the crystal. For neutrons which are faster than this sound velocity the contribution is independent of the neutron velocity and can be calculated using the formulae derived for X-ray scattering. However, for neutrons which are slower than the sound velocity the contribution is a function of the neutron velocity and will be less than that given by the X-ray formulae. The behaviour of the TDS contribution as a function of the neutron velocity is considered for a type scan for which an analytical evaluation is possible and these considerations are extended to the conventional ω and θ–2θ types of scan. It is concluded that there is no discontinuity in the TDS contribution when the velocity of the neutrons is the same as that of the phonons, but that evaluation of a reliable correction is difficult for slower-than-sound neutrons for the conventional types of scan. These conclusions will also apply for a more realistic case for which the phonon velocities are not all identical.

Introduction

We have discussed the correction of measured integrated Bragg intensities for thermal diffuse scattering (TDS) in a number of earlier papers (Cooper & Rouse, 1968; Rouse & Cooper, 1969, 1970; Cooper, 1970). In these papers we have, for the most part, considered the correction of X-ray diffraction data and we have touched only briefly on the corresponding correction of neutron diffraction data.

The theory for X-ray scattering is simplified by the fact that the energy of the X-rays is much larger than the energy of the phonons. This means that for X-rays we can approximate the scattering surfaces concerned to the Ewald sphere and a straightforward integration of the scattering cross section over the volume scanned in reciprocal space is then possible. On the other hand, for neutron scattering the energy of the neutrons is comparable with the energy of the phonons and the scattering surfaces no longer approximate to the Ewald sphere. Moreover, the form of the scattering surfaces is strongly dependent on the velocity of the neutrons, as has been discussed by Seeger & Teller (1942) for a one-velocity model, in which all phonons are assumed to have the same velocity. The one-phonon TDS cross-section for such a model has been discussed by Waller & Froman (1952), who derived expressions for this cross-section in the two cases of the neutrons being faster or slower than the phonons.

Willis (1970) has recently reconsidered this model, emphasizing the geometrical characteristics of the scattering of neutrons in reciprocal space and drawing certain conclusions in connexion with the correction of measured Bragg intensities for TDS. In particular he was able, from geometrical considerations, to draw certain qualitative conclusions concerning the TDS corrections for slower-than-sound neutrons. It is the purpose of the present paper to consider this one-velocity model in more detail and to derive expressions for the TDS intensity under normal experimental conditions. In addition, by considering a type of scan for which analytical evaluation is possible, it can be shown quantitatively how the correction necessary for the contribution of TDS to the Bragg intensities depends on the velocity of the neutrons. Although this simple model does not correspond to any real crystal it does provide a valuable insight into the behaviour of the TDS intensity near the reciprocal lattice point which can be applied in more realistic cases and it can be used to determine the conditions under which a reliable TDS correction can be calculated for a given crystal.

The correction of measured Bragg intensities for TDS using an isotropic model for the scattering has recently been reviewed by the author (Cooper, 1970). In the present paper I shall use essentially the same notation except that for the one-velocity model I shall replace $\mathbf{V}_j(\mathbf{q})$, the velocity of the phonon, by V_L (see Seeger & Teller, 1942) and in order to avoid confusion I shall consider the cross-section as a function of the wave-vector $\boldsymbol{\kappa}$, being the displacement of the termination of the wave-vector of the scattered neutron from the reciprocal-lattice point, rather than as a function of the wave-vector $\mathbf{q}$ of the created phonon (see Fig. 1). (The wave-vector $\mathbf{q}$ is $-\boldsymbol{\kappa}$ for a created phonon and $+\boldsymbol{\kappa}$ for an annihilated phonon.)

One-velocity scattering surfaces

The nature of the scattering surfaces for one-phonon scattering for a one-velocity model has been discussed by Seeger & Teller (1942), who show that the shape of these surfaces is defined by β, the ratio of the phonon velocity to the neutron velocity, V_n.

The changes in momentum and energy of the neutron are, respectively,

$$\pm \Delta p_S = |\mathbf{p}_i| - |\mathbf{p}_S| \quad (1)$$

$$\Delta E_n = V_n \Delta p_S \quad (2)$$

where $\mathbf{p}_i$ and $\mathbf{p}_S$ are the momenta of the incident and scattered neutrons respectively and we assume that $|\Delta \mathbf{p}_S| \ll |\mathbf{p}_i|$.

The conditions for scattering defined by equations (1) and (2) can be written in terms of the wave-vectors $\mathbf{k}_0$ and $\mathbf{k}$, for the incident and scattered neutron respectively, as

$$\frac{\Delta p_s}{p_L} = \frac{|\mathbf{k}_0| - |\mathbf{k}|}{|\boldsymbol{\kappa}|} = \frac{V_L}{V_n} = \beta \quad (3)$$

where p_L is the momentum of the phonon and $\boldsymbol{\kappa}$ is the vector:

$$\boldsymbol{\kappa} = \mathbf{k} - \mathbf{k}_0 - 2\pi\boldsymbol{\tau} \quad (4)$$

and $2\pi\boldsymbol{\tau}$ is the appropriate reciprocal-lattice vector.

Equation (3) defines a surface such that for any point on the surface the ratio of the distance of that point to the Ewald sphere to that of the point to the reciprocal-lattice point is β, the ratio of the phonon velocity to the neutron velocity. One-phonon scattering can only occur for scattered neutrons having wave-vectors $\mathbf{k}$ terminating on this surface.

Since only phonons with small wave-vectors contribute appreciably to the scattering we can approximate the Ewald sphere in the vicinity of the reciprocal-lattice point to a plane. Under these conditions the scattering surface will have the following properties.

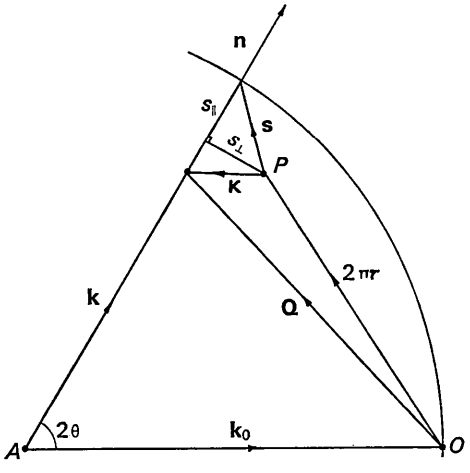

Fig. 1. Vector diagram in reciprocal space for a one-phonon scattering process involving loss of neutron energy and creation of a phonon. $\boldsymbol{\kappa}$ is the vector from the reciprocal lattice point P to the end of $\mathbf{k}$, the wave-vector of the scattered neutrons. $\mathbf{s}$ is the vector from P to the point at which the direction of $\mathbf{k}$ (unit vector $\mathbf{n}$) meets the Ewald sphere and $s_\parallel$ and $s_\perp$ are the components of s parallel to $\mathbf{n}$ and perpendicular to $\mathbf{n}$ respectively. For a scattering process involving gain in neutron energy and the annihilation of a phonon the diagram would be similar except that $\mathbf{k}$ and $2\pi\boldsymbol{\tau}$ would both terminate outside the Ewald sphere.

For faster-than-sound neutrons ($\beta < 1$) the scattering surface is a hyperboloid of two sheets, one on each side of the Ewald sphere. One sheet corresponds to phonon creation ($k < k_0$) and the other sheet corresponds to phonon annihilation ($k > k_0$); both these processes will occur simultaneously. As β goes to unity the surface becomes a paraboloid and for slower-than-sound neutrons ($\beta > 1$) it is an ellipsoid. For $\beta \geq 1$ the scattering corresponds to phonon creation only or to phonon annihilation only, depending on which side of the Ewald sphere the reciprocal-lattice point is.

Willis (1970) has discussed these geometrical properties in some detail and has given diagrams of scattering surfaces for $\beta = \frac{1}{2}$ and $\beta = 2$, corresponding to neutrons much faster or much slower than sound respectively. To illustrate the dependence of the scattering surfaces on the value of β three further diagrams are given here: Fig. 2(*a*) and (*b*) show the form of the scattering surfaces for β values close to unity, *viz.* $\frac{5}{6}$ and $\frac{10}{9}$, for various positions of the Ewald sphere with respect to the reciprocal-lattice point and Fig. 3 shows the form of the scattering surface for a single position of the Ewald sphere, for various values of β. For clarity Fig. 2(*a*) and (*b*) have been drawn with respect to a stationary Ewald sphere and considering the reciprocal-lattice point to move with respect to this.

The one-phonon scattering cross-section

(*a*) *Faster-than-sound neutrons* ($\beta < 1$)

We can rewrite the one-phonon scattering cross-section for phonons with wave-vector $\mathbf{q}$ [Cooper, 1970, equation (19)] as a function of $\boldsymbol{\kappa}$:

$$\left(\frac{d\sigma(\boldsymbol{\kappa})}{d\Omega}\right)_1 = \frac{NQ^2}{2m} \frac{k}{k_0} \sum_{j=1}^{3n} \frac{E_j(\mathbf{q}) \pm \frac{1}{2}\hbar\omega_j(\mathbf{q})}{|J_j(\boldsymbol{\kappa})|\omega_j^2(\mathbf{q})} |G_j(\mathbf{Q})|^2 \quad (5)$$

where N is the number of unit cells, each of mass m, $\mathbf{Q}$ is the scattering vector ($=\mathbf{k} - \mathbf{k}_0$), $E_j(\mathbf{q})$ and $\omega_j(\mathbf{q})$ are the energy and frequency respectively of the jth mode with wave-vector $\mathbf{q}$, $G_j(\mathbf{Q})$ is the 'structure factor for one-phonon scattering' and $|J_j(\boldsymbol{\kappa})|$ is the Jacobian which can be expressed as

$$|J_j(\boldsymbol{\kappa})| = 1 \pm \frac{\mathbf{k} \cdot \mathbf{V}_L}{|k| V_n} . \quad (6)$$

For low-frequency modes, which provide the major contribution to the cross-section, the structure factor G is equal to the structure factor for Bragg scattering F multiplied by $\cos \alpha_j(\mathbf{q})$, where $\alpha_j(\mathbf{q})$ is the angle between the scattering vector and the polarization direction of the mode concerned:

$$G_j(\mathbf{Q}) = F(\mathbf{Q}) \cos \alpha_j(\mathbf{q}) . \quad (7)$$

For a one-velocity model we can immediately sum the cross-section over the three low-frequency acoustic modes and so rewrite equation (5) in the form:

$$\left(\frac{d\sigma(\boldsymbol{\kappa})}{d\Omega}\right)_1 = \frac{NQ^2}{2m\kappa^2} |F(\mathbf{Q})|^2 \frac{k_B T}{|J(\boldsymbol{\kappa})| V_L^2} \quad (8)$$

assuming also that $k \simeq k_0$ and that we are considering only the classical region for which each mode has an energy k_BT, where k_B is the Boltzmann constant and T is the absolute temperature.

For a given direction of $\mathbf{k}$, which we can define by the unit vector $\mathbf{n}$, there will be two values of $\boldsymbol{\kappa}$ for which one-phonon scattering of faster-than-sound neutrons will occur. It can be shown (Waller & Froman, 1952) that the total scattering cross-section for these two contributions is:

$$\left(\frac{d\sigma(\mathbf{k}_0,\mathbf{n})}{d\Omega}\right)_1 = \frac{NQ^2|F(\mathbf{Q})^2|k_BT}{ms^2V_L^2} \qquad (9)$$

where $\mathbf{s}=|\mathbf{k}_0|\mathbf{n}-\mathbf{k}_0-2\pi\boldsymbol{\tau}$, *i.e.* the vector from the reciprocal-lattice point to the point at which the direction of the wave-vector of the scattered neutron crosses the Ewald sphere. For a scan through a reciprocal-lattice point $\mathbf{s}$ is therefore a vector defining the displacement from the Bragg condition.

We may note that, although the contributions from the individual $\boldsymbol{\kappa}s$ are dependent on the neutron velocity, the total cross-section, given by equation (9), is in fact independent of the neutron velocity and has an identical form to the corresponding result for X-ray scattering, for which $\boldsymbol{\kappa}_1=\boldsymbol{\kappa}_2=\mathbf{s}$.

It is convenient to rewrite equation (9) in the form:

$$\left(\frac{d\sigma(\mathbf{s})}{d\Omega}\right)_1 = \frac{2\sigma_0}{s^2} \qquad (10)$$

where

$$\sigma_0 = \frac{NQ^2|F(\mathbf{Q})|^2k_BT}{2m\,V_L^2}\,. \qquad (11)$$

(*b*) *Slower-than-sound neutrons* ($\beta>1$)

For slower than sound neutrons the scattering surface is an ellipsoid on the same side of the Ewald sphere as P. Summation of equation (8) over the two $\boldsymbol{\kappa}$ values for which scattering can occur for a given $\mathbf{n}$ then gives a total cross-section:

$$\left(\frac{d\sigma(\mathbf{s})}{d\Omega}\right)_1 = \frac{2\sigma_0}{s^2}\,\frac{\beta}{\sqrt{1-(\beta^2-1)\,(s_\perp/s_\parallel)^2}} \qquad (12)$$

(see Waller & Froman, 1952) where $s_\perp$ and $s_\parallel$ are the components of the scan vector $\mathbf{s}$, perpendicular to $\mathbf{n}$ and parallel to $\mathbf{n}$ respectively.

Since $\beta>1$ the cross section can be finite only for $s_\perp \le b$, where

$$b=(s_\perp)_{\max}=s_\parallel/\sqrt{\beta^2-1}\,, \qquad (13)$$

the semi minor axis of the ellipsoid.

Hence, for a given $s_\parallel$, the TDS is restricted to a limited range of $s_\perp$ values, corresponding to the size of the ellipsoid. For small $\bar{\mathbf{s}}$ it can be shown that the semi-angle subtended by the ellipsoid at the detctor is

$$\alpha=\sin 2\theta_B\,.\,\delta\theta/\sqrt{\beta^2-1} \qquad (14)$$

(see Lowde, 1954) where θ_B is the Bragg angle and $\delta\theta$ is the angle through which the crystal has been rotated from the Bragg setting.

TDS intensity

For a given setting of the diffractometer the total TDS intensity will be that given by integrating the cross-

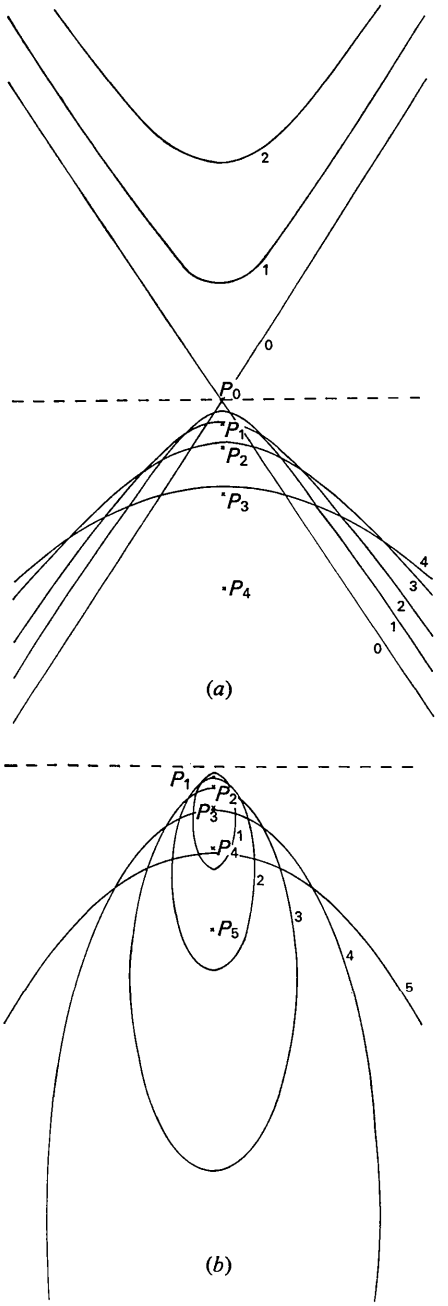

Fig. 2. The form of the scattering surfaces for one-phonon scattering of neutrons for various positions of the reciprocal-lattice point P with respect to the Ewald sphere and for various values of β: (*a*) $\beta=\frac{5}{6}$, and (*b*) $\beta=\frac{1}{9}$. The scattering surfaces are numbered to correspond with the appropriate position of P.

section over the probability function corresponding to the resolution of the instrument (see Cooper & Nathans, 1968*a*, 1968*b*). Under normal circumstances the major contribution to the resolution will arise from the finite aperture of the detector and in the present analysis we shall therefore consider the resolution function to be unity over the solid angle seen by the detector at a given setting and zero elsewhere. Neglect of the other contributions to the resolution will not affect the conclusions which can be drawn from the analysis.

(*a*) *Faster-than-sound neutrons* ($\beta < 1$)

We have seen that the one-phonon scattering cross section for faster-than-sound neutrons is identical in form to that derived for X-rays. The total one-phonon scattering for a given setting is thus obtained by integrating equation (9) over all **s** vectors from the reciprocal-lattice point which terminate on the part of the Ewald sphere seen by the detector at that setting. Hence the total one-phonon intensity measured during a scan through a Bragg reflexion is given by integrating equation (9) over the volume in reciprocal space for which elastic scattering can be detected during the scan. Methods available for carrying out this integration have been discussed elsewhere (see *e.g.* Cooper, 1970) and the results will take the same form as for X-ray scattering.

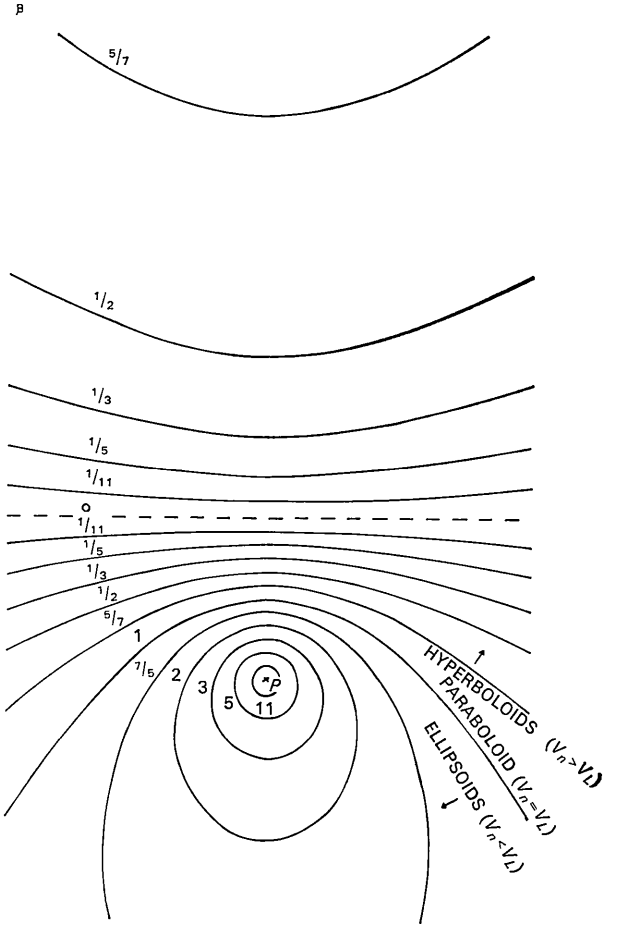

Fig. 3. The form of the scattering surfaces for one-phonon scattering of neutrons for a given position of the Ewald sphere with respect to the reciprocal-lattice point *P* for various values of β.

(*b*) *Slower-than-sound neutrons* ($\beta > 1$)

For slower-than-sound neutrons the cross-section is a more complicated function of **s** and depends also on the velocity of the neutrons. Scattering will only occur within a region subtending a cone of semi-angle α, given by equation (14), at the detector, *i.e.* the cone subtended by the ellipsoidal scattering surface. The observed TDS is therefore very critically dependent on what part, if any, of the ellipsoid is seen by the detector.

We have seen that the size of the ellipsoid decreases as β increases and that the ellipsoid contracts onto the Bragg peak as the displacement from the Bragg setting decreases. Hence there will be a finite range of scan over which the whole of the ellipsoid is seen by the detector. If we integrate equation (12) over the whole of the ellipsoid we obtain an integrated intensity of

$$I_N = \sigma_0 \, 4\pi \tanh^{-1}(1/\beta) \qquad (15)$$

(see Lowde, 1954).

We may note that this expression is independent of the displacement from the Bragg setting. Hence we have the result that, if β is sufficiently large for the whole of the ellipsoid to remain within the aperture of the detector throughout the scan, the TDS intensity remains constant. The normal background correction will then remove the whole of the TDS intensity and no further correction will be necessary.

If β is close to unity the ellipsoid will be larger for a given displacement from the Bragg setting (see Fig. 3) so that the ellipsoid may rapidly extend beyond the region seen by the detector. Thus the TDS intensity will remain constant over a small angular range only and the intensity will then decrease as an increasing fraction of the ellipsoid extends beyond the aperture of the detector. Hence the relative contribution of TDS to the background-corrected Bragg intensity will be the same as for X-rays for $\beta < 1$ but will fall to zero in a region of β greater than 1. In the following sections we shall consider the TDS contribution for particualr types of scan in order to determine how the TDS intensity depends on the value of β and the parameters of the scan.

Types of scan

We shall consider three types of scan through a Bragg reflexion: an ω scan, a θ–2θ scan and a perpendicular ($\perp$) scan, in which the end of the scattering vector for elastic scattering moves perpendicular to the Ewald sphere. These scans are illustrated in Fig. 4. At the Bragg setting the reciprocal-lattice point *P* lies on the

Ewald sphere. If AE is the vector in the same direction as the wave-vector of the scattered neutrons and terminating on the Ewald sphere, E, then coincides with P. During a scan E will move along the lines indicated: to E_0 for a perpendicular scan, E_1 for an ω scan and E_2 for a θ–2θ scan. A will also move perpendicular to OA, but for small $\delta\theta$ we can ignore the movement of A.

The apparent displacement of the centre of the ellipsoid from the centre of the detector aperture will correspond to the component of the displacement of E from P, normal to AP, viz.

for an ω scan,

$$d_1 = E_0E_1 = 2k \sin^2\theta\, \delta\theta \qquad (16a)$$

for a θ–2θ scan,

$$d_2 = E_0E_2 = -2k \cos^2\theta\, \delta\theta \qquad (16b)$$

and for a $\perp$ scan,

$$d_0 = 0\,. \qquad (16c)$$

For a rectangular aperture in which the Bragg reflexion is centred the detector will accept scattering within horizontal and vertical angles of $\pm v$ and $\pm w$ respectively with respect to the direction of the Bragg reflected beam. Hence for a given displacement from the Bragg setting the TDS intensity is given by integrating equation (12) over $s_\perp$ values lying within the vertical limits $\pm kw$ and the horizontal limits:

$$\begin{aligned} -2k \sin^2\theta\, \delta\theta \pm kv &\quad \text{for an } \omega \text{ scan,} \\ 2k \cos^2\theta\, \delta\theta \pm kv &\quad \text{for a } \theta\text{–}2\theta \text{ scan,} \end{aligned}$$

and

$$\pm kv \quad \text{for a } \perp \text{ scan.}$$

The intensity will be constant as long as the whole of the ellipsoid is seen by the detector, so that the condition for constant intensity is that the short axis of the ellipsoid [equation (13)] plus the displacement of the centre should be less than the maximum displacement accepted by the aperture, *i.e.*

$$\delta\theta < w\sqrt{\beta^2 - 1}\,/\sin 2\theta \qquad (17)$$

and

$$\delta\theta = v/[2 \sin^2\theta + (\sin 2\theta/\sqrt{\beta^2 - 1})] \text{ for an } \omega \text{ scan} \qquad (18a)$$

$$\delta\theta = v/[2 \cos^2\theta + (\sin 2\theta/\sqrt{\beta^2 - 1})] \text{ for a } \theta\text{–}2\theta \text{ scan} \qquad (18b)$$

or

$$\delta\theta < v\sqrt{\beta^2 - 1}/\sin 2\theta \text{ for a } \perp \text{ scan}\,. \qquad (18c)$$

Outside these ranges of $\delta\theta$ the detector will not see all the ellipsoid and intensity will be lost. The range is clearly largest for a perpendicular scan, for which the centre of the ellipsoid remains stationary with respect to the aperture of the detector. The change in the detector aperture for this type of scan is

$$\Delta(2\theta) = 2 \sin^2\theta\,.\,\delta\theta \qquad (19)$$

so that we can represent this scan as a θ–$(\sin^2\theta)2\theta$ scan. This is not normally a straightforward type of scan to use in practice but we shall see that its consideration allows an analytical determination of the TDS intensity observed during a scan to be made if an appropriate aperture is used.

Rectangular aperture

The integrated intensity for slower-than-sound neutrons is given by equation (15) until the displacement from the Bragg setting becomes large enough for the ellipsoid to extend beyond the detector aperture. It then becomes necessary to integrate equation (12) only over those values of $s_\perp$ which are seen by the detector.

If the ellipsoid is centred, the intensity obstructed by one vertical edge of the aperture for a given $s_\perp$ ($> kv$) is

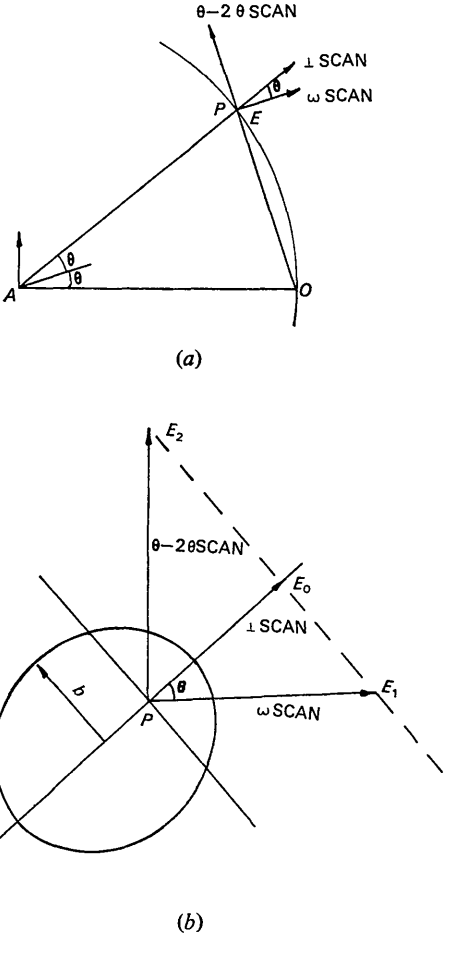

Fig. 4. Diagram in reciprocal space showing how the termination of the wave-vector for elastically scattered neutrons accepted by the detector moves during various types of scan through a Bragg reflexion. (*a*) General vector diagram. (*b*) Enlargement of the area close to the reciprocal- lattice point, showing also an ellipsoidal scattering surface of semi minor axis *b*.

$$\delta I_N = \frac{2}{s_\parallel^2} \times \frac{\beta 2\pi s_\perp}{\{1+(s_\perp^2/s_\parallel^2)\}\sqrt{1-\{(\beta^2-1)s_\perp^2/s_\parallel^2\}}} \times \frac{\sec^{-1}(s_\perp/kv)}{\pi}. \quad (20)$$

This must be integrated over $s_\perp$ from kv to $(s_\perp)_{\max}$ to give the total obstructed intensity

$$\Delta I_N = \sigma_0 \int_{\frac{kv}{(s_\perp)_{\max}\sqrt{\beta^2-1}}}^{\frac{1}{\sqrt{\beta^2-1}}} \frac{4\beta x \sec^{-1}\left(\frac{(s_\perp)_{\max}\sqrt{\beta^2-1}}{kv}x\right)}{(1+x^2)\sqrt{1-(\beta^2-1)x^2}}\,dx \quad (21)$$

where $x = s_\perp/s_\parallel$.

This analysis can be extended to the case of an ellipsoid displaced horizontally from the centre of the aperture and obstructed by any part of the rectangular aperture. The intensity for such a case is

$$\begin{aligned} I_N = {} & 4\pi\sigma_0 \tanh^{-1}(1/\beta) \\ & -\sigma_0\int_{\gamma_1}^{\varepsilon_1} \frac{4\beta x \sec^{-1}(x/\gamma_1)dx}{(1+x^2)\sqrt{1-(\beta^2-1)x^2}} \\ & -\sigma_0\int_{\gamma_2}^{\varepsilon_2} \frac{4\beta x \sec^{-1}(x/\gamma_2)dx}{(1+x^2)\sqrt{1-(\beta^2-1)x^2}} \\ & -2\sigma_0\int_{\delta}^{\varepsilon_1} \frac{4\beta x \sec^{-1}(x/\delta)dx}{(1+x^2)\sqrt{1-(\beta^2-1)x^2}} \\ & -\sigma_0\int_{\varepsilon_1}^{\varepsilon_2} \frac{4\beta x[\pi/2+\sec^{-1}(x/\varepsilon_1)]dx}{(1+x^2)\sqrt{1-(\beta^2-1)x^2}} \\ & -\sigma_0\int_{\varepsilon_2}^{X} \frac{4\pi\beta x dx}{(1+x^2)\sqrt{1-(\beta^2-1)x^2}} \end{aligned} \quad (22)$$

where the acceptance angles of the aperture are $\pm v$ horizontal and $\pm w$ vertical, d is the horizontal displacement of the ellipsoid from the centre of the aperture,

$$\gamma_1 = \frac{kv-d}{\sqrt{\beta^2-1(s_\perp)^2_{\max}}} \qquad \gamma_2 = \frac{kv+d}{\sqrt{\beta^2-1(s_\perp)^2_{\max}}}$$

$$\varepsilon_1 = \sqrt{\frac{(kv-d)^2+(kw)^2}{(\beta^2-1)\,(s_\perp)^2_{\max}}} \qquad \varepsilon_2 = \sqrt{\frac{(kv+d)^2+(kw)^2}{(\beta^2-1)\,(s_\perp)^2_{\max}}}$$

and

$$\delta = \frac{kw}{\sqrt{\beta^2-1\,(s_\perp)^2_{\max}}} \qquad X = \frac{1}{\sqrt{\beta^2-1}} \quad (23)$$

provided that these values are less than X. If any of these values are greater than X the appropriate γ, δ or ε must be replaced by X.

It is clear that numerical methods are necessary to evaluate equation (22) and that such a procedure will be necessary for every individual example. In order to obtain some quantitative results which are readily applicable to a range of experimental conditions we shall therefore consider a model for which analytical integration of equation (12) is possible, *viz.* a perpendicular scan with a circular aperture.

Perpendicular scan with a circular aperture

(*a*) *Intensity at a given setting*

For slower-than-sound neutrons the size of the ellipsoid will depend on $\delta\theta$, the displacement from the Bragg setting, but if a perpendicular scan is used it will remain centred in the aperture. If a circular aperture is used the intensity will remain constant until the ellipsoid first fills the aperture, after which the intensity will decrease.

If the angular radius of the aperture is v_0 then the intensity is

$$I_N = 4\pi\sigma_0 \tanh^{-1}(1/\beta) \quad (24)$$

for $(s_\perp)_{\max} \le kv_0$, and

$$I_N = 4\pi\sigma_0[\tanh^{-1}(1/\beta) - \tanh^{-1}(\sqrt{1-\gamma_0^2}/\beta)] \quad (25)$$

for $(s_\perp)_{\max} > kv_0$ and $\gamma_0 = kv_0/(s_\perp)_{\max}$.

We can rewrite equation (25) in terms of $\delta\theta$:

$$I_N = 4\pi\sigma_0\left[\tanh^{-1}\left(\frac{1}{\beta}\right) - \tanh^{-1}\left(\frac{1}{\beta}\right)\sqrt{1-\frac{(\beta^2-1)v_0^2}{\sin^2 2\theta(\delta\theta)^2}}\right] \quad (26)$$

or in terms of $s_\parallel$:

$$I_N = 4\pi\sigma_0\left[\tanh^{-1}\left(\frac{1}{\beta}\right) - \tanh^{-1}\left\{\left(\frac{1}{\beta}\right)\sqrt{1-(\beta^2-1)\left(\frac{kv_0}{s_\parallel}\right)^2}\right\}\right]. \quad (27)$$

For convenience we shall consider the intensity as a function of $s_\parallel$, bearing in mind that this is a function of 2θ.

The one-phonon intensity for slower than sound neutrons is constant for scans up to $s_\parallel = kv_0\sqrt{\beta^2-1}$, after which the intensity decreases as $s_\parallel$ increases. Hence, for β close to unity the intensity is constant only over a very small angle and is large over this angle. As β increases the peak intensity falls and the range over which it remains constant increases. We shall consider as examples the cases of $\beta = 1{\cdot}2$, 2 and 4, putting

$$s_\parallel = fkv_0\sqrt{\beta^2-1} \quad (28)$$

and

$$I_N = 4\pi\sigma_0[N]. \quad (29)$$

Values of $s_\parallel/(kv_0)$ and N are given for various values

of f in Table 1 and N is also shown as a function of $s_{\parallel}/(kv_0)$ in Fig. 5.

Table 1. *Values of $s_{\parallel}/(kv_0)$ and N for various values of f for slower-than-sound neutrons*

	$\beta=1{\cdot}2$		$\beta=2$		$\beta=4$	
f	$s_{\parallel}/(kv_0)$	N	$s_{\parallel}/(kv_0)$	N	$s_{\parallel}/(kv_0)$	N
1·0	0·663	1·199	1·732	0·5493	3·873	0·2554
1·01	0·670	1·081	1·749	0·4792	3·912	0·2061
1·05	0·696	0·939	1·819	0·3956	4·067	0·1791
1·1	0·730	0·835	1·905	0·3379	4·260	0·1509
1·2	0·796	0·701	2·078	0·2656	4·648	0·1163
1·4	0·929	0·532	2·425	0·1840		
1·6	1·061	0·423	2·771	0·1374		
1·8	1·194	0·345	3·118	0·1068		
2·0	1·327	0·288	3·454	0·0857		
2·4	1·592	0·209				
3·0	1·990	0·138				
4·0	2·653	0·081				
6·0	3·980	0·037				

For comparison we may consider the same situation for faster-than-sound neutrons ($\beta<1$), for which the intensity is, from equation (10),

$$I_F=2\sigma_0\int_0^{kv_0}\frac{2\pi s_{\perp}(\mathrm{d}s_{\perp})}{s^2} \qquad (30a)$$

$$=2\pi\sigma_0\log[1+(kv_0/s_{\parallel})^2]\,. \qquad (30b)$$

We can then write equation (30b) in the form

$$I_F=4\pi\sigma_0[M] \qquad (31)$$

and compare the values of M, given in Table 2, directly with those of N for slower-than-sound neutrons. M is also plotted in Fig. 5 for comparison. We may note that, although the peak intensity decreases rapidly as β increases ($\beta>1$), the intensity is larger than that for faster-than-sound neutrons towards the end of the constant region and beyond. The intensity integrated over a scan will therefore not fall as rapidly as the peak intensity.

Table 2. *Values of M for various values of $s_{\parallel}/(kv_0)$ for faster-than-sound neutrons*

$s_{\parallel}/(kv_0)$	M	$s_{\parallel}/(kv_0)$	M
0·2	1·829	1·0	0·396
0·5	0·804	1·5	0·184
0·6	0·664	2·0	0·116
0·7	0·556	2·5	0·074
0·8	0·470	3·0	0·052
0·9	0·402	3·5	0·040

(*b*) *Intensity integrated over scan*

We shall consider a scan from the Bragg setting out to $s_{\parallel}=s_0$. The total one-phonon intensity integrated over this scan for faster-than-sound neutrons is then, from equation (30b),

$$I_s=2\pi\sigma_0\int_0^{s_0}\log[1+(kv_0/s_{\parallel})^2]\,(\mathrm{d}s_{\parallel}) \qquad (32)$$

$$=2\pi\sigma_0 s_0\,[\log(1+1/T^2)+(2/T)\tan^{-1}T] \qquad (33)$$

where $T=s_0/(kv_0)$.

For slower-than-sound neutrons the corresponding integrated intensity is, from equation (27),

$$I_0=4\pi\sigma_0\int_0^{s_0}\tanh^{-1}(1/\beta)\,(\mathrm{d}s_{\parallel})$$

$$-4\pi\sigma_0\int_{kv_0/\sqrt{\beta^2-1}}^{s_0}\tanh^{-1}\left(\frac{1}{\beta}\sqrt{1-(\beta^2-1)\left(\frac{kv_0}{s_{\parallel}}\right)^2}\right)(\mathrm{d}s_{\parallel}) \qquad (34)$$

for $s_0>kv_0/\sqrt{\beta^2-1}$.

For $s_0\leq kv_0/\sqrt{\beta^2-1}$ the intensity is given by the first term only, *i.e.*

$$I_0=4\pi\sigma_0 s_0\tanh^{-1}(1/\beta)\,. \qquad (35)$$

We shall therefore consider initially a scan out to the limit of the linear region (see Fig. 5) for which we can use equation (35). The corresponding intensity for the same scan range for faster-than-sound neutrons can be calculated from equation (33) and values of I_0 and I_s, divided by the factor $4\pi\sigma_0\,kv_0$, are given in Table 3 for various values of β, together with the ratio $s_0/(kv_0)$ which indicates the length of the constant intensity scan.

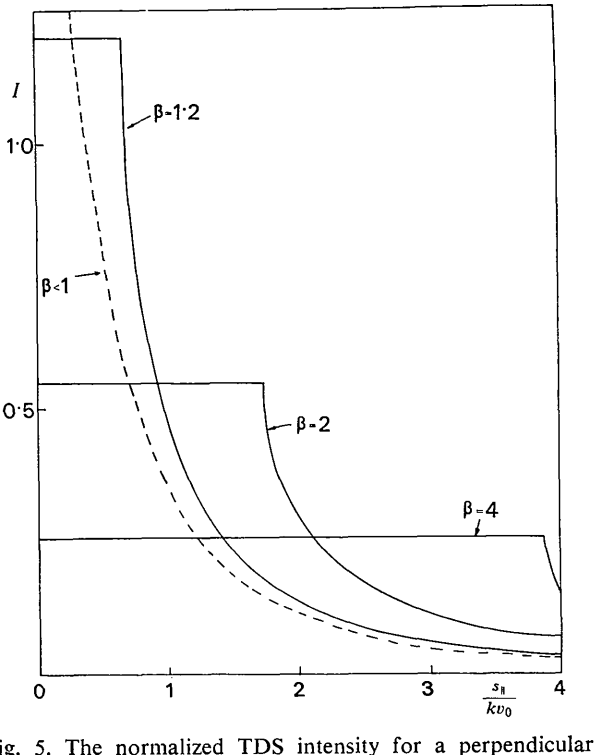

Fig. 5. The normalized TDS intensity for a perpendicular scan with a circular detector aperture as a function of $s_{\parallel}(kv_0)$ for various values of β for slower-than-sound neutrons (full curves) and for faster-than-sound neutrons (broken curve).

Table 3. *Normalized intensities and constant intensity scan range parameters for various values of* β

β	I_0	I_s	I_0/I_s	s_0/kv_0
1·001	0·170	0·184	0·924	0·045
1·01	0·377	0·421	0·896	0·14
1·02	0·464	0·525	0·884	0·20
1·05	0·595	0·690	0·862	0·32
1·1	0·697	0·830	0·840	0·46
1·2	0·791	0·974	0·812	0·66
2·0	0·951	1·296	0·734	1·73
4	0·989	1·443	0·685	3·87
10	0·998	1·520	0·657	9·95
∞	1·000	1·570	0·637	∞

In the limit as $\beta \to 1$, $I_0/I_s \to 1$, so that the intensity goes smoothly into that for $\beta < 1$; as the constant intensity region vanishes the peak intensity goes to infinity. In the slow neutron limit $\beta \to \infty$, $I_0/I_s \to 2/\pi$ as the intensity becomes infinite.

The scan range over which the intensity remains constant is strongly dependent on β and it is therefore more realistic to consider a fixed scan range. For convenience we shall consider $s_0' = 0{\cdot}46\ kv_0$, for which the intensity is constant if β is greater than 1·1. Normalized intensities (divided by the factor $4\pi\sigma_0 kv_0$) for this scan range are given in Table 4 and the value of I_0/I_s is plotted as a function of β in Fig. 6. The intensity, integrated over the scan, falls rapidly for $\beta > 1{\cdot}1$, when the constant region extends beyond the limit of the scan. It is therefore reasonable to suppose that the intensity for β between 1 and 1·1 joins the two calculated curves for β on either side of this range smoothly, as indicated in Fig. 6.

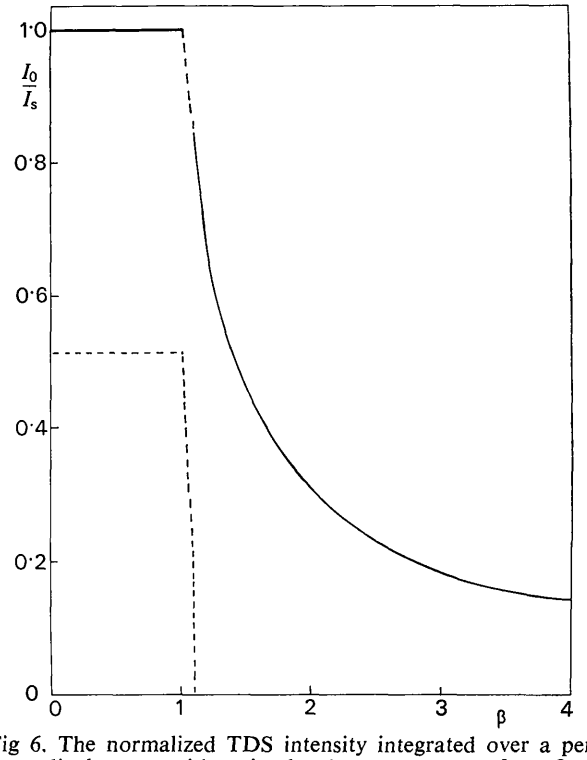

Fig 6. The normalized TDS intensity integrated over a perpendicular scan with a circular detector aperture for a fixed scan range, $s_0' = 0{\cdot}46\ kv_0$. Upper curve: intensity for a peak scan. Lower curve: intensity for a conventional background corrected scan.

Table 4. *Normalized integrated intensities for a fixed scan range,* $s_0' = 0{\cdot}46\ kv_0$, *for various values of* β

β	I_0	I_s	I_0/I_s
1·1	0·697	0·830	0·840
1·2	0·551	0·830	0·664
2·0	0·252	0·830	0·304
4	0·118	0·830	0·142
10	0·046	0·830	0·056
100	0·005	0·830	0·006
∞	0·000	0·830	0·000

Since the intensity remains constant over the whole scan for $\beta > 1{\cdot}1$, the TDS correction for a conventional background corrected Bragg intensity will then be zero. Hence the TDS correction must decrease rapidly between $\beta = 1$ and $\beta = 1{\cdot}1$ for this particular scan range. We should note also that the scan range is a function of 2θ, $s_0 = k \sin 2\theta \,.\, \Delta\theta$, and if the value of β is such that the constant intensity region does not fill the whole scan for some reflexions, the TDS correction may depend very critically on the value of 2θ.

From equation (30*b*) we have that for faster-than-sound neutrons the integrated TDS intensity for a conventional background correction is

$$I_B = 2\pi\sigma_0 s_0 \log[1 + (kv_0/s_0)^2] \qquad (36)$$

so that for $s_0 = 0{\cdot}46\ kv_0$, $I_B = 4\pi\sigma_0\, kv_0\,(0{\cdot}403)$. Hence the normalized background-corrected TDS intensity is $0{\cdot}830 - 0{\cdot}403 = 0{\cdot}427$ and $(I_s - I_B)/I_s = 0{\cdot}515$. For this scan range, therefore, the background corrected TDS falls from 51·5% of the value for the peak scan at $\beta = 1$ to zero at $\beta = 1{\cdot}1$, as indicated in Fig. 6. (The exact shape of this curve has not been calculated.) It is clear from this behaviour that, since the scan vector $\mathbf{s}_0$ is a function of the Bragg angle, the magnitude of the TDS correction for values of β in this region may vary rapidly from reflexion to reflexion.

ω and θ–2θ scans

For any other type of scan, *e.g.* ω or θ–2θ scans, the ellipsoid will move off the axis of the detector so that the constant intensity range will be shorter and the intensity will fall more rapidly. Hence the range of β for which the TDS correction is finite will be larger and more dependent on 2θ, since the rate at which the ellipsoid moves across the aperture also depends on θ [see equations (16)].

The displacement of the ellipsoid perpendicular to $s_{\parallel}$ is given from equations (16) as

$$|d| = 2k(\sin/\cos)2\theta \,.\, \delta\theta \qquad (37)$$

where we must take $\sin^2\theta$ for an ω scan and $\cos^2\theta$ for a θ–2θ scan.

The limit of the constant intensity range is therefore given by

$$2k(\sin/\cos)^2\theta \,.\, \Delta\theta + (k \sin 2\theta \,.\, \Delta\theta/\sqrt{\beta^2-1}) = kv_0 \tag{38}$$

so that

$$\theta\Delta = \frac{v_0}{2(\sin/\cos)^2\theta + (\sin 2\theta/\sqrt{\beta^2-1})} \,. \tag{39}$$

As $\delta\theta$ increase beyond this limit the intensity will fall and will reach zero if the ellipsoid becomes completely outside the aperture, *i.e.* when

$$\Delta\theta' = \frac{v_0}{2(\sin/\cos)^2\theta - (\sin 2\theta/\sqrt{\beta^2-1})} \,. \tag{40}$$

If the radius of the ellipsoid is increasing faster than the displacement the intensity will never fall to zero. Hence, the condition for the intensity to fall to zero is

$$\sin 2\theta < 2\sqrt{\beta^2-1}\,(\sin/\cos)^2\,\theta \tag{41}$$

which gives

$$(\cot/\tan)\,\theta < \sqrt{\beta^2-1} \tag{42}$$

where the condition is on cot θ for an ω scan and on tan θ for a θ–2θ scan.

As an example we can consider $\beta = 1{\cdot}4$ for which the intensity falls to zero for $\theta > 45°$ for an ω scan and for $\theta < 45°$ for a θ–2θ scan. For larger values of β the critical angles diverge, giving larger ranges for which the intensity falls to zero; for smaller values of β the ranges become smaller. We should note that, unless the scan lies within the constant intensity range defined by equation (39) it may be rather difficult to calculate a value for the TDS correction. Moreover, it is clear that for typical scan ranges this condition will only be satisfied for limited angular ranges for ω and θ–2θ scans, whatever the value of $\beta(\beta > 1)$.

Conclusions

(*a*) *Faster-than-sound neutrons* ($\beta < 1$)

For faster-than-sound neutrons the TDS correction has the same form as that for X-rays, provided that the conditions are such that the basic assumptions are still valid. We may therefore use the formulae derived for X-ray scattering for calculating the corrections in this case.

(*b*) *Slower-than-sound neutrons* ($\beta > 1$)

For slower-than-sound neutrons the scattering surface is an ellipsoid and the TDS intensity is constant until the ellipsoid projects outside the detector aperture. For a perpendicular [θ–(sin^2 θ)2θ] scan the range over which the intensity is constant increases from zero at $\beta = 1$ to infinity at $\beta = \infty$. However, the peak intensity also decreases and the intensity integrated over the constant intensity region decreases, as β increases from unity, and reaches the limit of $2/\pi$ times the intensity for faster-than-sound neutrons ($\beta < 1$), integrated to infinity. If the scan is restricted to the constant intensity region the TDS correction for a conventional background-corrected scan will be zero. However, because the scan vector is a function of the Bragg angle, there will be a critical region of β over which the correction will be extremely dependent on θ. This will be particularly so for ω or θ–2θ scans for which the ellipsoid is displaced from the centre of the aperture. For these scans the range of constant intensity will be smaller and the correction will be finite over a larger range of β. Moreover, since the displacement of the ellipsoid is also a function of the Bragg angle there will be a limited range of θ for which the ellipsoid remains within the detector aperture and the TDS intensity may fall to zero if both the displacement and β are large.

The basic conclusion is that there is no discontinuity in the contribution of thermal diffuse scattering to the intensity measured during a scan through a Bragg reflexion when the velocity of the neutrons is the same as that of the phonons concerned ($\beta = 1$). However, it is likely to be difficult to calculate accurate corrections in the region of β slightly greater than 1. For large values of β the TDS correction will be zero for a perpendicular scan. However, for the conventional ω and θ–2θ types of scan there will be ranges of Bragg angle for which the correction is finite and again its value will be difficult to determine.

It should be emphasized that the above considerations are based on a one-velocity model, which assumes that all phonons concerned have the same velocity in the crystal. This is, of course, quite unrealistic, but the results obtained do indicate the behaviour of the TDS intensity as a function of neutron velocity and Bragg angle and can be used to predict conditions under which reliable TDS corrections can be calculated for a given crystal. For example, if a neutron wavelength is chosen such that the neutrons are faster than all possible phonons in the crystal, TDS corrections can be calculated using the formulae derived for X-ray scattering. The critical wavelength, corresponding to the maximum phonon velocity, will depend on the elastic properties of the crystal and will normally lie in the range 0·8 to 2 Å. (In general this wavelength will be longer for soft materials than for hard materials.) The critical wavelength is thus normally in the range commonly used for Bragg intensity measurements. If accurate structure factors are required a neutron wavelength should therefore be chosen so that reliable TDS corrections can be calculated.

It is a pleasure to acknowledge numerous discussions with my colleague K. D. Rouse.

References

COOPER. M. J. (1970). *Thermal Neutron Diffraction.* Edited by B. T. M. WILLIS. Ch. 4. Oxford Univ. Press.

COOPER, M. J. & NATHANS, R. (1968*a*). *Acta Cryst.* A**24**, 481.
COOPER, M. J. & NATHANS, R. (1968*b*). *Acta Cryst.* A**24**, 619.
COOPER, M. J. & ROUSE, K. D. (1968). *Acta Cryst.* A**24**, 405.
LOWDE, R. D. (1954). *Proc. Roy. Soc.* A**221**, 206.
ROUSE, K. D. & COOPER, M. J. (1969). *Acta Cryst.* A**25**, 615.
ROUSE, K. D. & COOPER, M. J. (1970). *Acta Cryst.* A**26**, 457.
SEEGER, R. J. & TELLER, E. (1942). *Phys. Rev.* **62**, 37.
WALLER, I. & FROMAN, P. O. (1952). *Ark. Fys.* **4**, 183.
WILLIS, B. T. M. (1970). *Acta Cryst.* A**26**, 396.

Acta Cryst. (1971). A**27**, 157

Normal Probability Plot Analysis of Error in Measured and Derived Quantities and Standard Deviations

BY S. C. ABRAHAMS AND E. T. KEVE*

Bell Telephone Laboratories, Incorporated, Murray Hill, New Jersey, U.S.A.

(*Received* 25 *May* 1970)

Normal probability plot analysis is applied to independent sets of crystallographic structure factor measurements (F) and the derived coordinates (p). Differences between corresponding pairs of structure factors (ΔF) in the two sets are examined in terms of their pooled standard deviations (σF) by plotting the ordered statistic $\delta m = \Delta F/\sigma F$ against the expected normal distribution. Differences between pairs of coordinates (Δp) are similarly examined in a $\delta p = \Delta p/\sigma p$ half-normal probability plot. Both plots result in linear arrays of unit slope and zero intercept, for normal error distribution in the experiment and the model and correctly assigned standard deviations. Analysis of departures from this ideal, especially when both plots are considered together, provides detailed information of the kinds of error in δm and in δp. By inference, the kinds of error in F and σF as well as in p and σp can be deduced. The normal probability plot $\delta R = |F_{meas}| - |F_{calc}|/\sigma F_{meas}$ should ideally also be linear, with unit slope and zero intercept. Deviations from ideal provide considerably more information than the conventional R values. Analysis of δR in combination with δm plots allows further specification of the error distribution. Examples using these plots are given and discussed, based both on real and on simulated data.

Introduction

The association of a given measured quantity with a reliable estimate of the uncertainties in that quantity is of fundamental importance. The uncertainties in derived quantities, however, have often been given greater importance than those assigned to observed quantities. Propagation of error theory shows that estimates of these two kinds of uncertainty, later referred to as the derived and the assigned standard deviations respectively, are functionally related (for a discussion, see Birge, 1939). The additional dependence of the least-squares refined parameters on the weights of the observations, obtained from the assigned standard deviations, was implied by Gauss (1809). The assigned standard deviations are therefore critical, and should be estimated with care. Both these uncertainties should be capable of satisfying stringent *post facto* tests for validity.

The increasing use in structural crystallography of diffractometers to measure structure factors (F_{meas}) has stimulated attempts at assigning experimental standard deviations (σF_{meas}) to these quantities. Thus, Busing & Levy (1957) proposed an expression for σF_{meas} that included both counting statistics and an empirical term proportional to the net count in the reflection. Similar proposals have subsequently been made by others. An objective assessment of σF_{meas} on the same scale as the F_{meas} is, however, possible only from the sum of all the independent variances entering the measurement. A method for evaluating these variances has been given (Abrahams, 1964). The assigned σF_{meas} magnitudes are shown by model-dependent indicators to be close to their absolute scale (Abrahams, 1969).

In any model-independent procedure for testing the assigned standard deviations, it is necessary to measure at least two independent sets of F_{meas}. The availability of two independent data sets, which need not be complete, allows the validity both of the derived as well as the assigned standard deviations to be tested by methods developed below. In addition, duplicate measurements on two different crystals of the material under study considerably increase the chances that the crystallographic results reported are indeed typical of that material.

The results from a recent structural investigation (Keve, Abrahams & Bernstein, 1970), and a parallel simulated case, are used as examples to illustrate the

* Present address: Mullard Research Laboratories, Redhill, Surrey, England.